

A fitted L-Multi-point Flux Approximation method for pricing options

Rock Stephane Koffi, Antoine Tambue

Received: date / Accepted: date

Abstract In this paper, we introduce a special kind of finite volume method called Multi-Point Flux Approximation method (MPFA) to price European and American options in two dimensional domain. We focus on the L-MPFA method for space discretization of the diffusion term of Black-Scholes operator. The degeneracy of the Black Scholes operator is tackled using the fitted finite volume method. This combination of fitted finite volume method and L-MPFA method coupled to upwind methods gives us a novel scheme called the fitted L-MPFA method. Numerical experiments show the accuracy of the novel fitted L-MPFA method comparing to well known schemes for pricing options.

Keywords Finite volume methods, L Multi-Point Flux Approximation, Degenerated PDEs, Option pricing
MSC codes: 65M08, 68W25, 65C20

1 Introduction

In finance, an option is a contract which gives to the holder the right but not the obligation to buy (call) or to sell (put) an asset at a specific price (strike) at a certain date in the future (expiry date). We have two main types of options which are European and American options. European options are options that can be exercised only at expiry date while American options can be exercised anytime before the expiry date. This flexibility of exercising American options leads to solve an optimal stopping time problem in the Black-Scholes framework which incorporate the early exercise. Many studies focused on the pricing problem of American options were conducted and the linear complementary problem approach was quite popular for pricing American options (see Kovalov et al. [2007], Topper [2005], Wang et al. [2006], Zhang et al. [2009]). This approach brings us to solve linear complementary problem stated as follows (see Topper [2005]):

A. Tambue (Corresponding author)
Western Norway University of Applied Sciences, Inndalsveien 28, 5063 Bergen, Norway,
The African Institute for Mathematical Sciences(AIMS), 6-8 Melrose Road, Muizenberg 7945, South Africa
Center for Research in Computational and Applied Mechanics (CERECAM), and Department of Mathematics and Applied Mathematics, University of Cape Town, 7701 Rondebosch, South Africa.
Tel.: +47 55 58 70 06, E-mail: antonio@aims.ac.za, antoine.tambue@hvl.no, tambuea@gmail.com

R.S. Koffi
The African Institute for Mathematical Sciences(AIMS) of South Africa
Department of Mathematics and Applied Mathematics, University of Cape Town, 7701 Rondebosch, South Africa
E-mail: rock@aims.ac.za

$$\begin{cases} \mathcal{L}V & \geq 0 \\ V - V^* & \geq 0 \\ \mathcal{L}V \cdot (V - V^*) & = 0 \end{cases} \quad (1)$$

where \mathcal{L} is the following Black-Scholes operator

$$\mathcal{L}V = \frac{\partial V}{\partial \tau} - \frac{1}{2} \sum_{i,j=1}^n \sigma_i \sigma_j \rho_{ij} S_i S_j \frac{\partial^2 V}{\partial S_i \partial S_j} - r \sum_{i=1}^n S_i \frac{\partial V}{\partial S_i} + rV \quad (2)$$

with r is the risk free interest, V is the option value at time τ , V^* is the payoff, $\tau = T - t$ with t and T respectively the instantaneous and maturity time. For $i, j = 1, \dots, n$, S_i represents the asset i price, σ_i represents the volatility of asset i , ρ_{ij} represents the correlation between the assets i and j .

Furthermore, Wang et al. [2006] proposed a power penalty method to solve the linear complementary problem for pricing American options. The power penalty problem is formulated as follows:

$$\mathcal{L}V + \beta [V^* - V]_+^{1/k} = 0 \quad (3)$$

where β is penalty parameter and k is the power of the method. Let us notice that, when we take the penalty parameter $\beta = 0$ in (3), we get the Black-scholes Equation for pricing European options, with the operator \mathcal{L} defined in (2). However, the power penalty problem (3) can not be solved analytically, therefore numerical methods are required for its resolution. Nevertheless, the Black-Scholes operator (2) is degenerated when the stock price approaches zero. This degeneracy can affect the accuracy of the numerical method used for the resolution. To tackle this problem, several methods have been proposed. The fitted finite volume method, proposed by S.Wang in Wang [2004] whereby a rigorous proof of convergence is provided, appears to be more attractive. Moreover, the fitted finite volume method has been used for the resolution of the two dimensional second order Black Scholes PDE followed by the convergence proof in Huang et al. [2006]. In spite of the fact that the fitted finite volume methods perform well for the resolution of the Black Scholes PDE, they are only of order 1 with respect to asset price variable. Besides, the fitted O-Multi-Point Flux Approximation (O-MPFA) method has been proposed in Koffi and Tambue [2019] to overcome the degeneracy problem of the Black-Scholes PDE. It has been shown that the O-MPFA is more accurate than the classical fitted finite volume method by Wang [2004]. However, the O-MPFA is heavy (9 points stencil method) and for more general grids, the convergence rate of the O-MPFA method may reduce (see Aavatsmark [2007]).

In this paper, we focus on the L-MPFA method which is based on the approximation of a linear function gradient defined over a given triangle and the continuity of flux through the edges of this triangle.

Indeed, the L-MPFA method is a 7 points stencil method while the O-MPFA is a 9 points stencil method. This shows that the O-MPFA method can be computationally more expensive than the L-MPFA method. Moreover, for more general grids, the order reduction in convergence rate is larger for the O-MPFA than the L-MPFA (see Aavatsmark [2002]). Thereby, to approximate the solution of the second order Black Scholes operator, we couple the L-MPFA method with the upwind methods (first and second order). Besides, the degeneracy of the Black Scholes operator (2) is handled by the fitted finite volume ,Wang [2004], when the stock price is approaching zero. The L-MPFA method coupled with the upwind methods (1^{st} and 2^{nd} order) is used to approximate the solution of (3) when the Black operator is not degenerated. We call fitted L-MPFA method that combination of the L-MPFA method and the fitted finite volume method. Numerical simulations show that the new fitted L-MPFA method is more accurate than the fitted O-MPFA method developed in Koffi and Tambue [2019] and the standard fitted finite volume method developed in Huang et al. [2006].

The paper is structured as follows. In section 2, we present the power penalty problem with the corresponding initial and boundary conditions. The spatial discretization of the linear operator is developed in the section 3. Details on the L-MPFA method of the diffusion term discretization are provided. The convection term is discretized using the upwind methods (1^{st} and 2^{nd} method). At the end of the section 3, the novel fitted MPFA method is provided. The θ - Euler method is used for the time discretization method in the section 4. Numerical experiments are presented for the different numerical methods are presented in the section 5. The conclusions of our study are drawn in the last section.

2 Formulation of the problem

2.1 Option with two underlying assets

Pricing an American option with 2 underlying assets leads to solve the following power penalty problem:

$$\mathcal{L}V + \beta[V^* - V]_+^{1/k} = 0 \quad (4)$$

where the Black-Scholes operator is defined as:

$$\mathcal{L}V = \frac{\partial V}{\partial \tau} - \frac{1}{2}\sigma_1^2 x^2 \frac{\partial^2 V}{\partial x^2} - \rho\sigma_1\sigma_2 xy \frac{\partial^2 V}{\partial x \partial y} - \frac{1}{2}\sigma_2^2 y^2 \frac{\partial^2 V}{\partial y^2} - rx \frac{\partial V}{\partial x} - ry \frac{\partial V}{\partial y} + rV \quad (5)$$

with the following initial and boundary conditions

$$\begin{cases} V(x, y, 0) = V^*(x, y) = \max(K - \alpha_1 x - \alpha_2 y, 0) \\ V(0, y, \tau) = V(x, 0, \tau) = K \\ \lim_{x, y \rightarrow +\infty} V(x, y, \tau) = 0 \end{cases} \quad (6)$$

with K the strike price, V^* the payoff for basket options and α_i , $i = 1, 2$, are weights such that $\alpha_1 + \alpha_2 = 1$.

When the penalty parameter $\beta = 0$ in (4), we get the Black-Scholes Partial Differential Equation for pricing European options with the corresponding initial and boundary conditions

$$\begin{cases} V(x, y, 0) = V^*(x, y) = \max(K - \alpha_1 x - \alpha_2 y, 0) \\ V(0, y, \tau) = V(x, 0, \tau) = 0 \\ \lim_{x \rightarrow \infty} V(x, y, \tau) = x - Ke^{-r\tau} \\ \lim_{y \rightarrow \infty} V(x, y, \tau) = y - Ke^{-r\tau} \end{cases} \quad (7)$$

In order to apply the finite volume method, it is convenient to re-write the Black-Scholes operator (5) in the following divergence form

$$\frac{\partial V}{\partial \tau} - \nabla \cdot (\mathbf{M} \nabla V) - \nabla(fV) - \lambda V + \beta[V^* - V]_+^{1/k} = 0 \quad (8)$$

where

$$\mathbf{M} = \frac{1}{2} \begin{pmatrix} \sigma_1^2 x^2 & \rho\sigma_1\sigma_2 xy \\ \rho\sigma_1\sigma_2 xy & \sigma_2^2 y^2 \end{pmatrix}, f = \begin{pmatrix} (r - \sigma_1^2 - \frac{1}{2}\rho\sigma_1\sigma_2)x \\ (r - \sigma_2^2 - \frac{1}{2}\rho\sigma_1\sigma_2)y \end{pmatrix}$$

$$\lambda = -3r + \sigma_1^2 + \sigma_2^2 + \rho\sigma_1\sigma_2$$

2.2 Finite volume method

Let us consider the new domain Ω of study by truncating D such that $\Omega = I_x \times I_y \times [0, T]$ where $I_x = [0, x_{\max}]$ and $I_y = [0, y_{\max}]$. In the sequel of this work, the Black-Scholes operator (5) is considered over the truncated domain Ω .

At $x = x_{\max}$ and $y = y_{\max}$, the linear boundary condition will be applied Huang et al. [2006]. The intervals I_x and I_y will be subdivided into N in the following way Huang et al. [2006] Huang et al. [2009] without loss the generality.

$$I_{x_i} = [x_{i-1}; x_i], \quad I_{y_j} = [y_{j-1}; y_j] \quad i, j = 1, \dots, N + 1. \quad (9)$$

Let us set the mid-points $x_{i-\frac{1}{2}}$ and $y_{j-\frac{1}{2}}$ as follows

$$x_{i-\frac{1}{2}} = \frac{x_{i-1} + x_i}{2} \quad y_{j-\frac{1}{2}} = \frac{y_{j-1} + y_j}{2} \quad i, j = 1, \dots, N, \quad (10)$$

with $h_i = x_{i+\frac{1}{2}} - x_{i-\frac{1}{2}}$, $l_j = y_{j+\frac{1}{2}} - y_{j-\frac{1}{2}}$ and

$$x_{-\frac{1}{2}} = x_0 = 0, \quad x_{N+\frac{3}{2}} = x_{N+1} = x_{\max}, \quad y_{-\frac{1}{2}} = y_0 = 0, \quad y_{N+\frac{3}{2}} = y_{N+1} = y_{\max}.$$

For $i, j = 1, \dots, N + 1$, we denote by $\mathcal{C}_{ij} = [x_{i-\frac{1}{2}}; x_{i+\frac{1}{2}}] \times [y_{j-\frac{1}{2}}; y_{j+\frac{1}{2}}]$ a control volume associated our subdivision.

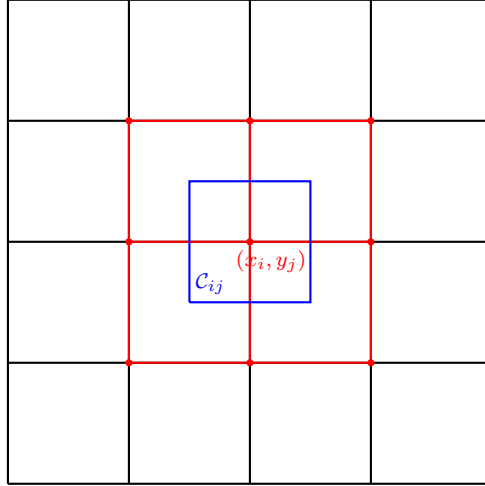


Fig. 1: Control volume

Note that for $i, j = 1, \dots, N$ the control volume \mathcal{C}_{ij} is the area surrounding the grid point (x_i, y_j) .

Our goal is to approximate the option function V at (x_i, y_j) ¹ by a function denoted \mathcal{V} .

The matrix \mathbf{M} in (8) will be replaced by its average value in each control volume

$$\mathbf{M}^{ij} = \frac{1}{\text{meas}(\mathcal{C}_{ij})} \int_{\mathcal{C}_{ij}} \mathbf{M} dx dy, \quad i, j = 1, \dots, N. \quad (11)$$

¹ center of the control volume \mathcal{C}_{ij}

where $\text{meas}(\mathcal{C}_{ij})$ is the measure of \mathcal{C}_{ij} . Thereby, we have

$$M^{ij} = \begin{bmatrix} \frac{\sigma_1^2}{6} \frac{x_{i+\frac{1}{2}}^3 - x_{i-\frac{1}{2}}^3}{x_{i+\frac{1}{2}} - x_{i-\frac{1}{2}}} & \frac{\rho\sigma_1\sigma_2}{8} (x_{i+\frac{1}{2}} + x_{i-\frac{1}{2}})(y_{j+\frac{1}{2}} + y_{j-\frac{1}{2}}) \\ \frac{\rho\sigma_1\sigma_2}{8} (x_{i+\frac{1}{2}} + x_{i-\frac{1}{2}})(y_{j+\frac{1}{2}} + y_{j-\frac{1}{2}}) & \frac{\sigma_2^2}{6} \frac{y_{j+\frac{1}{2}}^3 - y_{j-\frac{1}{2}}^3}{y_{j+\frac{1}{2}} - y_{j-\frac{1}{2}}} \end{bmatrix}$$

Now let us consider the divergence form given in (8). According to the finite volume method, we integrate the partial differential equation (8) over each control volume \mathcal{C}_{ij} . For $i, j = 1, \dots, N$, we have:

$$\int_{\mathcal{C}_{ij}} \frac{\partial \mathcal{V}}{\partial \tau} d\mathcal{C} - \int_{\mathcal{C}_{ij}} \nabla \cdot (\mathbf{M}\nabla \mathcal{V}) d\mathcal{C} - \int_{\mathcal{C}_{ij}} \nabla(f\mathcal{V}) d\mathcal{C} - \int_{\mathcal{C}_{ij}} \lambda \mathcal{V} d\mathcal{C} + \int_{\mathcal{C}_{ij}} \beta [V^* - \mathcal{V}]_+^{1/k} d\mathcal{C} = 0 \quad (12)$$

The next section will be dedicated to spatial discretization of equation (12). For the term in the left hand side of the equality sign and for the last one in the right hand side of (12), we use the mid-point quadrature rule for their approximation as follows:

$$\int_{\mathcal{C}_{ij}} \frac{\partial \mathcal{V}}{\partial \tau} d\mathcal{C} \approx \text{meas}(\mathcal{C}_{ij}) \frac{\partial \mathcal{V}}{\partial \tau}(x_i, y_j, \tau) \approx h_i l_j \frac{\partial \mathcal{V}_{ij}}{\partial \tau} \quad (13)$$

$$\int_{\mathcal{C}_{ij}} \lambda \mathcal{V} d\mathcal{C} \approx \text{meas}(\mathcal{C}_{ij}) \lambda \mathcal{V}(x_i, y_j, \tau) \approx h_i l_j \lambda \mathcal{V}_{ij} \quad (14)$$

$$\int_{\mathcal{C}_{ij}} \beta [V^* - \mathcal{V}]_+^{1/k} d\mathcal{C} \approx \text{meas}(\mathcal{C}_{ij}) \beta [V^* - \mathcal{V}]_+^{1/k} \approx h_i l_j \beta [V_i^* - \mathcal{V}_{ij}]_+^{1/k} \quad (15)$$

the convection term

$$\int_{\mathcal{C}_{ij}} \nabla(f\mathcal{V}) d\mathcal{C} \quad (16)$$

of (12) will be approximated using the upwind methods (first or second order).

The diffusion term

$$\int_{\mathcal{C}_{ij}} \nabla \cdot (\mathbf{M}\nabla \mathcal{V}) d\mathcal{C} \quad (17)$$

of (12) will be approximated using the **Multi-Point Flux Approximation (MPFA) L-method** or the **fitted multi-point flux approximation L-method**. More details about these methods will be given in the next section.

3 Space discretization

The spatial discretization of (8) consists in approximating all terms in (12) over the control volumes of the spatial domain.

3.1 Discretization of the diffusion term

Let us start by applying the divergence theorem to the diffusion term (17) as follows, for $i, j = 1, \dots, N$:

$$\mathcal{F}^{ij} = \int_{\mathcal{C}_{ij}} \nabla \cdot (\mathbf{M}^{ij} \nabla \mathcal{V}) = \int_{\partial \mathcal{C}_{ij}} (\mathbf{M}^{ij} \nabla \mathcal{V}) \cdot \mathbf{n} d\partial \mathcal{C} \quad (18)$$

where \mathbf{n} is the outward vector from the control volume.

Now, we can apply the so-called **L-Multi-Point Flux Approximation(MPFA)** method to approximate the integral defined in (18).

3.1.1 L -Multi-Point Flux Approximation (L-MPFA) method

The L-MPFA method takes its name from the fact that the curve connecting the three control volume centres considered for the application of the method, constitutes a stylized "L". Here, we follow the description of the L-method given in Aavatsmark [2002].

Let us consider the triangle $x_1 x_2 x_3$ (see Figure 2), and a linear function g defined over this triangle. we define

$$\mathbf{X} \nabla g = \begin{bmatrix} g(x_2) - g(x_1) \\ g(x_3) - g(x_1) \end{bmatrix} \quad (19)$$

where

$$\mathbf{X} = \begin{bmatrix} (x_2 - x_1)^T \\ (x_3 - x_1)^T \end{bmatrix} \quad (20)$$

Thereby, the gradient of the linear function g may be expressed as follows:

$$\nabla g = \frac{1}{T} \left(\nu_2 (g(x_2) - g(x_1)) + \nu_3 (g(x_3) - g(x_1)) \right) \quad (21)$$

where ν_2, ν_3 are respectively the normal vector to $x_2 - x_1$ and $x_3 - x_1$ defined by

$$\nu_2 = \mathbf{R}(x_2 - x_1), \quad \nu_3 = -\mathbf{R}(x_3 - x_1)$$

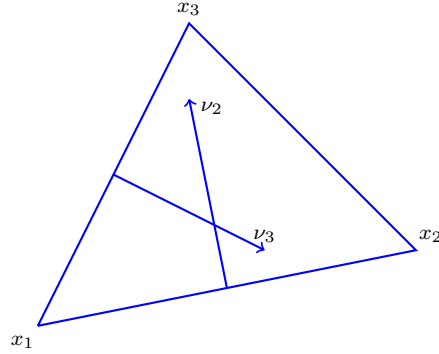
with

$$\mathbf{R} = \begin{bmatrix} 0 & 1 \\ -1 & 0 \end{bmatrix}$$

and

$$T = \nu_2^T \mathbf{R} \nu_3$$

Let's notice that the matrix \mathbf{R} is a rotation of angle $-\frac{\pi}{2}$. Thereby the vector ν_2 and ν_3 have same length with the vectors $x_2 - x_1$ and $x_3 - x_1$.

Fig. 2: Triangle $x_1x_2x_3$

Let us call **interaction volume** \mathcal{R}_{ij} a cell grid defined as follows

$$\text{for } i, j = 1, \dots, N+1 \quad \mathcal{R}_{ij} = [x_{i-1}; x_i] \times [y_{j-1}; y_j] \quad (22)$$

We denote respectively by $x_1(x_{i-1}, y_{j-1})$, $x_2(x_i, y_{j-1})$, $x_3(x_i, y_j)$ and $x_4(x_{i-1}, y_j)$ the centre of the control volume \mathcal{C}_{ij} , $\mathcal{C}_{i+1,j}$, $\mathcal{C}_{i,j+1}$ and $\mathcal{C}_{i+1,j+1}$. We denote also by \bar{x}_1 , \bar{x}_2 , \bar{x}_3 and \bar{x}_4 the midpoints of the segment x_1x_2 , x_3x_4 , x_1x_3 and x_2x_4 . We may notice that an interaction volume \mathcal{R}_{ij} , for $i, j = 1, \dots, N+1$, is covering an area in the intersection of the control volumes \mathcal{C}_{ij} , $\mathcal{C}_{i+1,j}$, $\mathcal{C}_{i,j+1}$ and $\mathcal{C}_{i+1,j+1}$. An interaction volume can be divided into 2 triangles such that the half edges 1, 2 are in the triangle $T_1 = x_1x_2x_3$ and the half edges 3, 4 are in the triangle $T_2 = x_1x_3x_4$ (see Figure 3).

Here, We follow the procedure in Aavatsmark [2007].

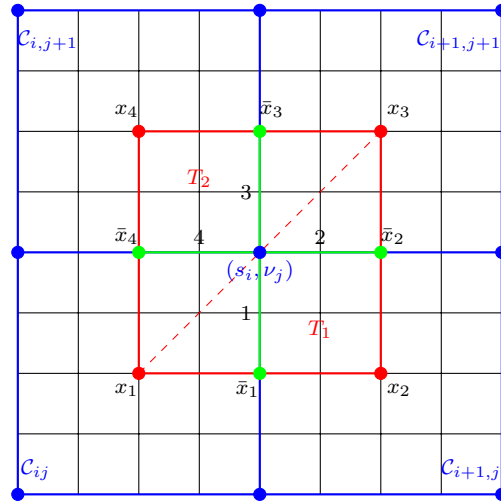


Fig. 3: Interaction volume

In an interaction volume, we aim to compute the flux through the half edges 1, 2, 3 and 4 (See 3).

Thereby, using (18), the flux f_p^{ij} through the half edge p seen from the centre of the control volume \mathcal{C}_{ij} is expressed as follows:

$$f_p^{ij} = n_p^T \mathbf{M}^{ij} \nabla \mathcal{V}_{ij} \quad (23)$$

where n_p is the vector normal to the half edge p with the same length.

Let us consider the triangle $T_1 = x_1x_2x_3$ from the interaction volume \mathcal{R}_{ij}

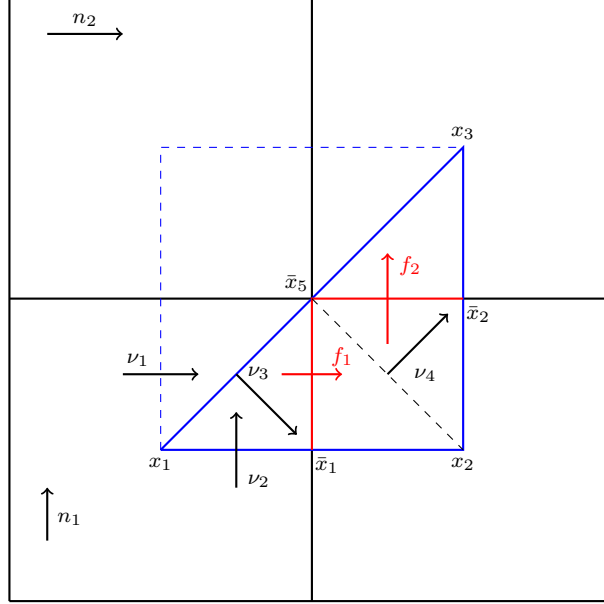


Fig. 4: Triangle T_1

In the triangle $T_{12} = \bar{x}_1x_2\bar{x}_2$, using the flux expression (23) and following the gradient expression in (21) we get

$$\begin{aligned} f_1^{i,j-1} &= \omega_{12}^{i,j-1} (\bar{\mathcal{V}}_2 - \mathcal{V}_{i,j-1}) - \omega_{11}^{i,j-1} (\bar{\mathcal{V}}_1 - \mathcal{V}_{i,j-1}) \\ f_2^{i,j-1} &= \omega_{22}^{i,j-1} (\bar{\mathcal{V}}_2 - \mathcal{V}_{i,j-1}) - \omega_{21}^{i,j-1} (\bar{\mathcal{V}}_1 - \mathcal{V}_{i,j-1}) \end{aligned} \quad (24)$$

where

$$\begin{aligned} \omega_{11}^{i,j-1} &= \frac{1}{T_1^{i,j-1}} \times n_1^T \mathbf{M}^{i,j-1} \nu_1 & \omega_{12}^{i,j-1} &= \frac{1}{T_1^{i,j-1}} \times n_1^T \mathbf{M}^{i,j-1} \nu_2 \\ \omega_{21}^{i,j-1} &= \frac{1}{T_1^{i,j-1}} \times n_2^T \mathbf{M}^{i,j-1} \nu_1 & \omega_{22}^{i,j-1} &= \frac{1}{T_1^{i,j-1}} \times n_2^T \mathbf{M}^{i,j-1} \nu_2 \end{aligned}$$

with

$$T_1^{i,j-1} = -\nu_2^T \mathbf{R} \nu_1$$

Moreover, using the property of the matrix \mathbf{R} , we have

$$\nu_4 = \mathbf{R}(\bar{x}_5 - x_2) \quad (25)$$

Using also the equation (19) and the expression of gradient (21) in the triangle T_{12} lead to

$$\bar{\mathcal{V}}_5 = \mathcal{V}_{i,j-1} + \chi_{42}^{i,j-1} (\bar{\mathcal{V}}_2 - \mathcal{V}_{i,j-1}) - \chi_{41}^{i,j-1} (\bar{\mathcal{V}}_1 - \mathcal{V}_{i,j-1}) \quad (26)$$

where

$$\chi_{41}^{i,j-1} = \frac{1}{T_1^{i,j-1}} \nu_4^T \mathbf{R} \nu_1 \quad \chi_{42}^{i,j-1} = \frac{1}{T_1^{i,j-1}} \nu_4^T \mathbf{R} \nu_2$$

In the triangle $T_{11} = x_1 \bar{x}_1 \bar{x}_5$, we have

$$f_1^{i-1,j-1} = \omega_{13}^{i-1,j-1} (\bar{\mathcal{V}}_1 - \mathcal{V}_{i-1,j-1}) + \omega_{12}^{i-1,j-1} (\bar{\mathcal{V}}_5 - \mathcal{V}_{i-1,j-1}) \quad (27)$$

Replacing $\bar{\mathcal{V}}_5$ by its expression (26) in (27), we have

$$f_1^{i-1,j-1} = \omega_{13}^{i-1,j-1} (\bar{\mathcal{V}}_1 - \mathcal{V}_{i-1,j-1}) + \omega_{12}^{i-1,j-1} \left(\mathcal{V}_{i,j-1} - \mathcal{V}_{i-1,j-1} + \chi_{42}^{i,j-1} (\bar{\mathcal{V}}_2 - \mathcal{V}_{i,j-1}) - \chi_{41}^{i,j-1} (\bar{\mathcal{V}}_1 - \mathcal{V}_{i,j-1}) \right) \quad (28)$$

where

$$\omega_{13}^{i-1,j-1} = \frac{1}{T_1^{i-1,j-1}} \times n_1^T \mathbf{M}^{i-1,j-1} \nu_3 \quad \omega_{12}^{i-1,j-1} = \frac{1}{T_1^{i-1,j-1}} \times n_1^T \mathbf{M}^{i-1,j-1} \nu_2$$

with

$$T_1^{i-1,j-1} = \nu_3^T \mathbf{R} \nu_2$$

Similarly, in the triangle $T_{13} = \bar{x}_5 \bar{x}_2 x_3$

$$f_2^{ij} = -\omega_{21}^{ij} (\bar{\mathcal{V}}_5 - \mathcal{V}_{ij}) + \omega_{23}^{ij} (\bar{\mathcal{V}}_2 - \mathcal{V}_{ij}) \quad (29)$$

Replacing $\bar{\mathcal{V}}_5$ by its expression (26) in (29), we have

$$f_2^{ij} = -\omega_{21}^{ij} \left(\mathcal{V}_{i,j-1} - \mathcal{V}_{ij} + \chi_{42}^{i,j-1} (\bar{\mathcal{V}}_2 - \mathcal{V}_{i,j-1}) - \chi_{41}^{i,j-1} (\bar{\mathcal{V}}_1 - \mathcal{V}_{i,j-1}) \right) + \omega_{23}^{ij} (\bar{\mathcal{V}}_2 - \mathcal{V}_{ij}) \quad (30)$$

where

$$\omega_{21}^{ij} = \frac{1}{T_1^{ij}} \times n_2^T \mathbf{M}^{ij} \nu_1 \quad \omega_{23}^{ij} = \frac{1}{T_1^{ij}} \times n_2^T \mathbf{M}^{ij} \nu_3$$

with

$$T_1^{ij} = -\nu_3^T \mathbf{R} \nu_3$$

Since the flux is continuous through edges, then using (24), (28) and (30) we have

$$\left\{ \begin{array}{l} f_1 = \omega_{12}^{i,j-1}(\bar{\mathcal{V}}_2 - \mathcal{V}_{i,j-1}) - \omega_{11}^{i,j-1}(\bar{\mathcal{V}}_1 - \mathcal{V}_{i,j-1}) \\ \quad = \omega_{13}^{i-1,j-1}(\bar{\mathcal{V}}_1 - \mathcal{V}_{i-1,j-1}) + \omega_{12}^{i-1,j-1} \left(\mathcal{V}_{i,j-1} - \mathcal{V}_{i-1,j-1} + \chi_{42}^{i,j-1}(\bar{\mathcal{V}}_2 - \mathcal{V}_{i,j-1}) - \chi_{41}^{i,j-1}(\bar{\mathcal{V}}_1 - \mathcal{V}_{i,j-1}) \right) \\ f_2 = \omega_{22}^{i,j-1}(\bar{\mathcal{V}}_2 - \mathcal{V}_{i,j-1}) - \omega_{21}^{i,j-1}(\bar{\mathcal{V}}_1 - \mathcal{V}_{i,j-1}) \\ \quad = -\omega_{21}^{ij} \left(\mathcal{V}_{i,j-1} - \mathcal{V}_{ij} + \chi_{42}^{i,j-1}(\bar{\mathcal{V}}_2 - \mathcal{V}_{i,j-1}) - \chi_{41}^{i,j-1}(\bar{\mathcal{V}}_1 - \mathcal{V}_{i,j-1}) \right) + \omega_{23}^{ij}(\bar{\mathcal{V}}_2 - \mathcal{V}_{ij}) \end{array} \right. \quad (31)$$

by setting

$$g = \begin{bmatrix} f_1 \\ f_2 \end{bmatrix}, \quad W = \begin{bmatrix} \mathcal{V}_{i-1,j-1} \\ \mathcal{V}_{i,j-1} \\ \mathcal{V}_{ij} \end{bmatrix}, \quad \mathcal{V} = \begin{bmatrix} \bar{\mathcal{V}}_1 \\ \bar{\mathcal{V}}_2 \end{bmatrix} \quad (32)$$

The system of equations (31) can be written as

$$g = C^{ij}\mathcal{V} + D^{ij}W \quad (33)$$

where

$$C^{ij} = \begin{bmatrix} -\omega_{11}^{i,j-1} & \omega_{12}^{i,j-1} \\ -\omega_{21}^{i,j-1} & \omega_{22}^{i,j-1} \end{bmatrix} \quad D^{ij} = \begin{bmatrix} 0 & \omega_{11}^{i,j-1} - \omega_{12}^{i,j-1} & 0 \\ 0 & \omega_{21}^{i,j-1} - \omega_{22}^{i,j-1} & 0 \end{bmatrix}$$

Using the expressions at both sides of the second equalities of system equations (31) we have

$$A^{ij}\mathcal{V} = B^{ij}W \quad (34)$$

$$A^{ij} = \begin{bmatrix} \omega_{11}^{i,j-1} + \omega_{13}^{i-1,j-1} - \omega_{12}^{i-1,j-1}\chi_{41}^{i,j-1} & -\omega_{12}^{i,j-1} + \omega_{12}^{i-1,j-1}\chi_{42}^{i,j-1} \\ \omega_{21}^{i,j-1} + \omega_{21}^{ij}\chi_{41}^{i,j-1} & -\omega_{22}^{i,j-1} + \omega_{23}^{ij} - \omega_{21}^{ij}\chi_{42}^{i,j-1} \end{bmatrix}$$

$$B^{ij} = \begin{bmatrix} \omega_{13}^{i-1,j-1} + \omega_{12}^{i-1,j-1} & -\omega_{12}^{i,j-1} + \omega_{11}^{i,j-1} - \omega_{12}^{i-1,j-1}(1 + \chi_{41}^{i,j-1} - \chi_{42}^{i,j-1}) & 0 \\ 0 & -\omega_{22}^{i,j-1} + \omega_{21}^{i,j-1} + \omega_{21}^{ij}(1 + \chi_{41}^{i,j-1} - \chi_{42}^{i,j-1}) & -\omega_{21}^{ij} + \omega_{23}^{ij} \end{bmatrix}$$

Thereby, by solving (34) with respect to \mathcal{V} and replacing in (33) we get

$$g = R^{ij}\mathcal{V} \quad (35)$$

where

$$R^{ij} = C^{ij}[A^{ij}]^{-1}B^{ij} + D^{ij}$$

Now considering the triangle T_2 (see figure 3) and applying the above procedure used in the triangle T_1 , we are able to the fluxes through the half edges 3 and 4 as follows:

$$h = S^{ij}V \quad (36)$$

where

$$h = \begin{bmatrix} f_3 \\ f_4 \end{bmatrix}, \quad V = \begin{bmatrix} \mathcal{V}_{i,j-1} \\ \mathcal{V}_{ij} \\ \mathcal{V}_{ij} \end{bmatrix}$$

For simplicity, in an interaction volume \mathcal{R}_{ij} , the flux through the half edges 1, 2, 3 and 4 are given by

$$f = T^{ij}\mathcal{V} \quad (37)$$

where

$$f = \begin{bmatrix} f_1 \\ f_2 \\ f_3 \\ f_4 \end{bmatrix}, \quad \mathcal{V} = \begin{bmatrix} \mathcal{V}_{i-1,j-1} \\ \mathcal{V}_{i,j-1} \\ \mathcal{V}_{ij} \\ \mathcal{V}_{i-1,j} \end{bmatrix} \quad (38)$$

and T^{ij} is 4×4 matrix coming from R^{ij} and S^{ij} defined in (35),(36). T^{ij} is called the transmissibility matrix of the interaction volume \mathcal{R}_{ij} .

Let us notice that the flux through a full edge will be the addition of the fluxes through its 2 half edges.

Let us recall that, from (18), our aim is to compute the flux through the edges of the control volume \mathcal{C}_{ij} . In order to cover the boundary of a control volume, we need to four interaction volumes

Let us denote, for the volume control \mathcal{C}_{ij} , by εf_l^{ij} the flux through lower half eastern edge, by εf_u^{ij} the flux through the upper half eastern edge. The flux εf^{ij} through the east edge of the control volume \mathcal{C}_{ij} is calculated as follows:

The lower half eastern edge is in position 3 in the triangle T_2 of the interaction volume $\mathcal{R}_{i+1,j}$ (See figure 4). So by using (37) we have:

$$\varepsilon f_l^{ij} = T_{31}^{i+1,j}\mathcal{V}_{i,j-1} + T_{33}^{i+1,j}\mathcal{V}_{i+1,j} + T_{34}^{i+1,j}\mathcal{V}_{ij}$$

Similarly, the upper half eastern edge is in position 1 in the triangle T_1 of the interaction volume $\mathcal{R}_{i+1,j+1}$ and it is in position 1 in the interaction volume. Thereby using ((37)) we have:

$$\varepsilon f_u^{ij} = T_{11}^{i+1,j+1}\mathcal{V}_{ij} + T_{12}^{i+1,j+1}\mathcal{V}_{i+1,j} + T_{13}^{i+1,j+1}\mathcal{V}_{i+1,j+1}$$

Finally the flux through the eastern edge of the control volume \mathcal{C}_{ij} will be the addition of εf_l^{ij} and εf_u^{ij} . Thereby we have:

$$\begin{aligned} \varepsilon f^{ij} &= \varepsilon f_d^{ij} + \varepsilon f_u^{ij} \\ \varepsilon f^{ij} &= T_{31}^{i+1,j}\mathcal{V}_{i,j-1} + \left(T_{33}^{i+1,j} + T_{12}^{i+1,j+1}\right)\mathcal{V}_{i+1,j} + \left(T_{11}^{i+1,j+1} + T_{34}^{i+1,j}\right)\mathcal{V}_{ij} + T_{13}^{i+1,j+1}\mathcal{V}_{i+1,j+1} \end{aligned} \quad (39)$$

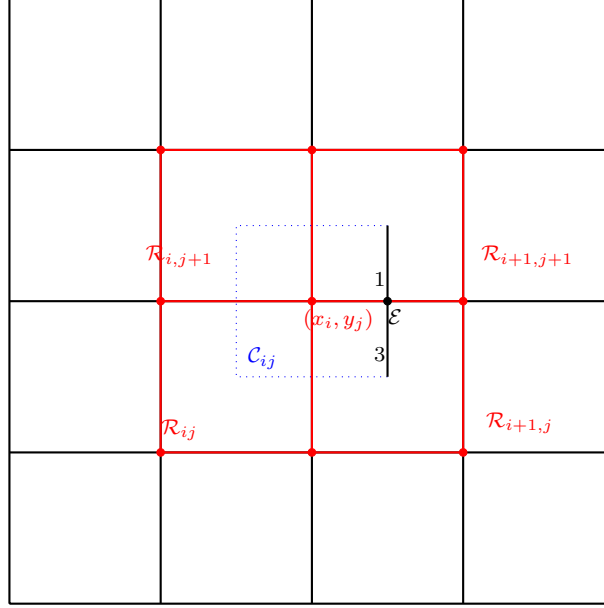


Fig. 5

The same method is applied to calculate the flux through the northern, western and southern edges of the control volume \mathcal{C}_{ij} . The flux through the edges of the control volume \mathcal{C}_{ij} is obtained by summing up the flux through the 4 edges. This gives :

$$\mathcal{F}_{ij} = a_{ij}\mathcal{V}_{ij} + b_{ij}\mathcal{V}_{i+1,j} + c_{ij}\mathcal{V}_{i+1,j+1} + d_{ij}\mathcal{V}_{i,j+1} + e_{ij}\mathcal{V}_{i-1,j} + \alpha_{ij}\mathcal{V}_{i-1,j-1} + \beta_{ij}\mathcal{V}_{i,j-1} \quad (40)$$

where

$$\begin{aligned} a_{ij} &= T_{11}^{i+1,j+1} + T_{34}^{i+1,j} + T_{41}^{i+1,j+1} + T_{22}^{i,j+1} - T_{12}^{i,j+1} - T_{33}^{ij} - T_{23}^{ij} - T_{44}^{i+1,j} \\ b_{ij} &= T_{33}^{i+1,j} + T_{12}^{i+1,j+1} - T_{43}^{i+1,j} & c_{ij} &= T_{13}^{i+1,j+1} + T_{43}^{i+1,j+1} & d_{ij} &= T_{23}^{i,j+1} + T_{44}^{i+1,j+1} - T_{13}^{i,j+1} \\ e_{ij} &= T_{21}^{i,j+1} - T_{11}^{i,j+1} - T_{34}^{ij} & \alpha_{ij} &= -T_{31}^{ij} - T_{21}^{ij} & \beta_{ij} &= T_{31}^{i+1,j} - T_{22}^{ij} - T_{41}^{i+1,j} \end{aligned}$$

This leads to a system of equations which can be written as follows:

$$\mathcal{F} = A_{mp}\mathcal{V} + F_{mp} \quad (41)$$

where

$$\mathcal{F} = \begin{bmatrix} \mathcal{F}_{11} \\ \mathcal{F}_{12} \\ \vdots \\ \mathcal{F}_{1N} \\ \mathcal{F}_{21} \\ \mathcal{F}_{22} \\ \vdots \\ \mathcal{F}_{NN} \end{bmatrix} \quad \mathcal{V} = \begin{bmatrix} \mathcal{V}_{11} \\ \mathcal{V}_{12} \\ \vdots \\ \mathcal{V}_{1N} \\ \mathcal{V}_{21} \\ \mathcal{V}_{22} \\ \vdots \\ \mathcal{V}_{NN} \end{bmatrix} \quad A_{mp} = \begin{bmatrix} W_1 & X_1 & 0_N & \dots & \dots & \dots & \dots & 0_N \\ Y_2 & W_2 & X_2 & \ddots & & & & \vdots \\ 0_N & Y_3 & W_3 & X_3 & \ddots & & & \vdots \\ \vdots & \ddots & Y_4 & W_4 & X_4 & \ddots & & \vdots \\ \vdots & & \ddots & \ddots & \ddots & \ddots & & \vdots \\ \vdots & & & \ddots & \ddots & \ddots & & 0_N \\ \vdots & & & & \ddots & Y_{N-1} & W_{N-1} & X_{N-1} \\ 0_N & \dots & \dots & \dots & \dots & 0_N & Y_N & W_N \end{bmatrix}$$

with 0_N is $N \times N$ zeros matrix, W_i, X_i, Z_i are tridiagonal matrix and F_{mp} is a N^2 vector coming from the boundary conditions.

The diffusion matrix A_{mp} is under the following form:

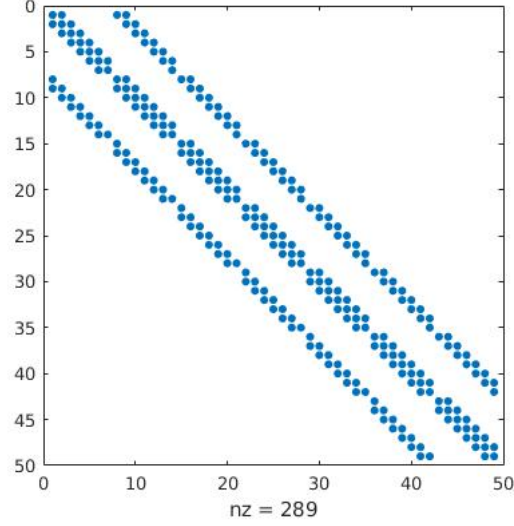


Fig. 6: A structure of the diffusion matrix using L-MPFA method.

As we can see on Fig.6, the L-MPFA method is a 7 points stencil method, unlikely to the O-MPFA method (see Koffi and Tambue [2019]) which is a 9 points stencil method.

3.2 Discretisation of the convection term

The integral of convection term

$$\int_{\mathcal{C}_{ij}} \nabla(f\mathcal{V})d\mathcal{C}$$

where

$$f = \begin{pmatrix} (r - \sigma_1^2 - \frac{1}{2}\rho\sigma_1\sigma_2)x \\ (r - \sigma_2^2 - \frac{1}{2}\rho\sigma_1\sigma_2)y \end{pmatrix}$$

will be approximated using the upwind methods (1^{st} and 2^{nd} order). We start by applying the divergence theorem, and we have for $i, j = 1, \dots, N$:

$$I^{ij} = \int_{\mathcal{C}_{ij}} \nabla(f\mathcal{V})d\mathcal{C}_{ij} = \int_{\partial\mathcal{C}_{ij}} (f \cdot \mathcal{V}) \cdot \mathbf{n}d\partial\mathcal{C}_{i,j} \quad (42)$$

with \mathbf{n} an outward unit normal vector.

3.2.1 First order upwind method

The **first order upwind method** discussed in [LeVeque, 2004, chapter 4.8] will be applied to evaluate the second term of (12).

I^{ij} is calculated by summing up the flux through the edges of the control volume \mathcal{C}_{ij} .

The flux through an edge using the first order upwind will depend on the sign of $f \cdot \mathbf{n}$ on this edge. If the sign of $f \cdot \mathbf{n}$ is positive, \mathcal{V}_{ij} will be used to approximate $(f \cdot \mathbf{n}\mathcal{V})$ otherwise we will use the value of \mathcal{V} in other side of the edge.

By doing so, we get $\forall i, j = 1, \dots, N$

$$I^{ij} = \epsilon_{ij}\mathcal{V}_{i-1,j} + \mu_{ij}\mathcal{V}_{i,j-1} + \Omega_{ij}\mathcal{V}_{ij} + \phi_{ij}\mathcal{V}_{i,j+1} + \Psi_{ij}\mathcal{V}_{i+1,j} \quad (43)$$

where

$$\epsilon_{ij} = -l_j f_x^{i-1} \max(f_x^{i-1}, 0); \quad \mu_{ij} = -h_i f_y^{j-1} \max(f_y^{j-1}, 0)$$

$$\Omega_{ij} = l_j \left(f_x^i \max(f_x^i, 0) - f_x^{i-1} \min(f_x^{i-1}, 0) \right) + h_i \left(f_y^j \max(f_y^j, 0) - f_y^{j-1} \min(f_y^{j-1}, 0) \right)$$

$$\phi_{ij} = h_i f_y^j \min(f_y^j, 0); \quad \Psi_{ij} = l_j f_x^i \min(f_x^i, 0)$$

Equation (43) will lead to a system of equations which be written as follows:

$$I = A_{up}\mathcal{V} + F_{up} \quad (44)$$

where A_{up} is a $M \times N$ matrix

$$I = \begin{bmatrix} I^{11} \\ I^{12} \\ \vdots \\ I^{1N} \\ I^{21} \\ I^{22} \\ \vdots \\ \vdots \\ I^{NN} \end{bmatrix} \quad \mathcal{V} = \begin{bmatrix} \mathcal{V}_{11} \\ \mathcal{V}_{12} \\ \vdots \\ \mathcal{V}_{1N} \\ \mathcal{V}_{21} \\ \mathcal{V}_{22} \\ \vdots \\ \vdots \\ \mathcal{V}_{NN} \end{bmatrix} \quad A_{up} = \begin{bmatrix} H_1 & P_1 & 0_N & \dots & \dots & \dots & 0_N \\ Q_2 & H_2 & P_2 & \ddots & & & \vdots \\ 0_N & Q_3 & H_3 & P_3 & \ddots & & \vdots \\ \vdots & \ddots & \ddots & \ddots & \ddots & \ddots & \vdots \\ \vdots & & \ddots & Q_{N-2} & H_{N-2} & P_{N-2} & 0_N \\ \vdots & & & \ddots & Q_{N-1} & H_{N-1} & P_{N-1} \\ 0_N & \dots & \dots & \dots & 0_N & Q_N & H_N \end{bmatrix}$$

with 0_N is $N \times N$ zeros matrix, H_i is a tridiagonal matrix, P_i, Q_i are diagonal matrices and F_{up} is a vector coming from the boundary conditions.

The advection matrix A_{up} using the first order upwind method is under following form

Therefore, combining the L-MPFA method (41) and the first order upwind (44), we get

$$\frac{d\mathcal{V}}{d\tau} = A\mathcal{V} + G(\mathcal{V}) + F \quad (45)$$

with

$$A = L^{-1} \left(A_{mp} + A_{up} + A_L \right) \quad G(\mathcal{V}) = \beta \left[\max(\mathcal{V}^* - \mathcal{V}, 0) \right]^{1/k} \quad F = L^{-1} \left(F_{mp} + F_{up} \right)$$

where A_L is a diagonal matrix of size $N \times N$ coming from the discretisation of (14). The diagonal elements of A_L are $A_{ii} = h_i l_i \lambda$ for $i = 1, \dots, N$ with λ given in (8). The matrix L is also a diagonal matrix of size $N \times N$ whose diagonal elements are $L_{ii} = h_i l_i$ for $i = 1, \dots, N$

3.2.2 Second order upwind method

A second order approximation is used to calculate the flux defined in (42). For instance, the flux εJ^{ij} through the eastern edge of the control volume \mathcal{C}_{ij} is approximated as follows: We will start by giving an approximation of the gradient in the integral expression (18).

$$\varepsilon J^{ij} = \int_{\mathcal{E}_{ij}} (f \cdot \mathcal{V}) \cdot n_{\varepsilon} \quad (46)$$

where

$$\mathbf{n}_{\varepsilon} = \begin{bmatrix} 1 \\ 0 \end{bmatrix}$$

is the outward unit normal vector to the eastern edge \mathcal{E}_{ij} of the control volume \mathcal{C}_{ij} . We set $f_x = f \cdot n_{\varepsilon}$ and we have

$$\mathcal{V} \approx \begin{cases} \frac{3\mathcal{V}_{ij} - \mathcal{V}_{i-1,j}}{2} & \text{if } f_x \geq 0 \\ \frac{3\mathcal{V}_{i+1,j} - \mathcal{V}_{i+2,j}}{2} & \text{if } f_x < 0 \end{cases} \quad (47)$$

Then we get

$$\varepsilon J^{ij} = l_j \left[\frac{3}{2} \max(f_x^{i+1}, 0) \mathcal{V}_{ij} - \frac{1}{2} \max(f_x^{i+1}, 0) \mathcal{V}_{i-1,j} + \frac{3}{2} \min(f_x^{i+1}, 0) \mathcal{V}_{i+1,j} - \frac{1}{2} \min(f_x^{i+1}, 0) \mathcal{V}_{i+2,j} \right] \quad (48)$$

with

$$f_x^{i+1} = (r - \sigma_x^2 - \frac{1}{2} \rho \sigma_x \sigma_y) x_{i+\frac{1}{2}}$$

We use the same argument to calculate the flux $_{\mathbb{N}}J^{ij}$, $_{\mathbb{W}}J^{ij}$, $_{\mathbb{S}}J^{ij}$ through the northern, western and southern edges of the control volume \mathcal{C}_{ij} and after sum them up. We get then

$$\begin{aligned} J^{ij} = & \epsilon_{ij} \mathcal{V}_{i-2,j} + \eta_{ij} \mathcal{V}_{i-1,j} + \kappa_{ij} \mathcal{V}_{i,j-2} + \mu_{ij} \mathcal{V}_{i,j-1} + \Omega_{ij} \mathcal{V}_{ij} + \phi_{ij} \mathcal{V}_{i,j+1} + \Psi_{ij} \mathcal{V}_{i,j+2} + \Delta_{ij} \mathcal{V}_{i+1,j} \\ & + \Pi_{ij} \mathcal{V}_{i+2,j} \end{aligned} \quad (49)$$

where

$$\begin{aligned}
\epsilon_{ij} &= \frac{1}{2} l_j \max(f_x^i, 0) & \eta_{ij} &= -\frac{1}{2} l_j \max(f_x^{i+1}, 0) - \frac{3}{2} l_j \max(f_x^i, 0) \\
\kappa_{ij} &= \frac{1}{2} h_i \max(f_y^j, 0) & \mu_{ij} &= -\frac{1}{2} h_i \max(f_y^{j+1}, 0) - \frac{3}{2} h_i \max(f_y^j, 0) \\
\Omega_{ij} &= \frac{3}{2} l_j \max(f_x^{i+1}, 0) + \frac{3}{2} h_i \max(f_y^{j+1}, 0) - \frac{3}{2} l_j \min(f_x^i, 0) - \frac{3}{2} h_i \min(f_y^j, 0) \\
\phi_{ij} &= \frac{3}{2} h_i \min(f_y^{j+1}, 0) + \frac{1}{2} h_i \min(f_y^j, 0) & \psi_{ij} &= -\frac{1}{2} h_i \min(f_y^{j+1}, 0) \\
\Delta_{ij} &= \frac{3}{2} l_j \min(f_x^{i+1}, 0) + \frac{1}{2} l_j \min(f_x^i, 0) & \Pi_{ij} &= -\frac{1}{2} l_j \min(f_x^{i+1}, 0)
\end{aligned}$$

For the control volumes near the boundary of the study domain, the first order upwind method is used for the approximation of the flux through edges directly connected to the boundary.

Equation (49) leads to a system of equations which can be written as:

$$J = A_{2up} \mathcal{V} + F_{2up} \quad (50)$$

where

$$J = \begin{bmatrix} J^{11} \\ J^{12} \\ \vdots \\ J^{1N} \\ J^{21} \\ J^{22} \\ \vdots \\ J^{NN} \end{bmatrix} \quad \mathcal{V} = \begin{bmatrix} \mathcal{V}_{11} \\ \mathcal{V}_{12} \\ \vdots \\ \mathcal{V}_{1N} \\ \mathcal{V}_{21} \\ \mathcal{V}_{22} \\ \vdots \\ \mathcal{V}_{NN} \end{bmatrix} \quad A_{2up} = \begin{bmatrix} K_1 & R_1 & G_1 & 0_N & \dots & \dots & 0_N \\ S_2 & K_2 & R_2 & G_2 & & \ddots & \vdots \\ H_3 & S_3 & K_3 & R_3 & G_3 & & \vdots \\ \vdots & \ddots & \ddots & \ddots & \ddots & \ddots & \vdots \\ \vdots & & H_{N-2} & S_{N-2} & K_{N-2} & R_{N-2} & G_{N-2} \\ \vdots & & & & H_{N-1} & S_{N-1} & K_{N-1} & R_{N-1} \\ 0_N & \dots & \dots & 0_N & H_N & S_N & K_N & R_N \end{bmatrix}$$

where for $i = 1, \dots, N$ K_i is penta-diagonal matrice and R_i, G_i, S_i, H_i are diagonal matrices. F_{2up} is a vector coming from the boundary conditions.

Therefore, combining the L-MPFA method (41) and the second order upwind method (50), we have

$$\frac{d\mathcal{V}}{d\tau} = A\mathcal{V} + G(\mathcal{V}) + F \quad (51)$$

with

$$A = L^{-1} \left(A_{mp} + A_{2up} + A_L \right) \quad G(\mathcal{V}) = \beta \left[\max(\mathcal{V}^* - \mathcal{V}, 0) \right]^{1/k} \quad F = L^{-1} \left(F_{mp} + F_{2up} \right)$$

where A_L is a diagonal matrix of size $N \times N$ coming from the discretisation of (14). The diagonal elements of

A_L are $A_{ii} = h_i l_i \lambda$ for $i = 1, \dots, N$ with λ given in (8). The matrix L is also a diagonal matrix of size $N \times N$ whose diagonal elements are $L_{ii} = h_i l_i$ for $i = 1, \dots, N$

Besides, the ellipticity condition for the PDE (2) is not satisfied when the stocks price ($x \rightarrow 0$ and/or $y \rightarrow 0$) is near to zero. This may cause some oscillations of the numerical solution when the PDE is degenerate. Nevertheless, Wang [2004] suggested a fitted finite volume method to deal with the degeneracy of the PDE. Thereby, the fitted finite volume method will be applied in the degeneracy region ($x \rightarrow 0$ and/or $y \rightarrow 0$) in the next section.

3.2.3 Fitted finite volume

The fitted finite volume method is used to approximated the flux through edges which are (fully) in the degeneracy region i.e the western edge of the control volume $\mathcal{C}_{1,j}$ $j = 1, \dots, N$ and the southern edge of the control volume $\mathcal{C}_{i,1}$ $i = 1, \dots, N$.

For the western edge of the control volume $\mathcal{C}_{1,j}$ $j = 1, \dots, N$, using the mid-quadrature rule, we have:

$$\int_{(x_{\frac{1}{2}}, y_{j-\frac{1}{2}})}^{(x_{\frac{1}{2}}, y_{j+\frac{1}{2}})} \left(m_{11} \frac{\partial \mathcal{V}}{\partial x} + m_{12} \frac{\partial \mathcal{V}}{\partial y} + p \mathcal{V} \right) dy \approx \left(m_{11} \frac{\partial \mathcal{V}}{\partial x} + m_{12} \frac{\partial \mathcal{V}}{\partial y} + p \mathcal{V} \right)_{(x_{\frac{1}{2}}, y_j)} \cdot l_j \quad (52)$$

besides, we have:

$$m_{11} \frac{\partial \mathcal{V}}{\partial x} + m_{12} \frac{\partial \mathcal{V}}{\partial y} + p \mathcal{V} = x \left(a x \frac{\partial \mathcal{V}}{\partial x} + d \frac{\partial \mathcal{V}}{\partial y} + b \mathcal{V} \right) \quad (53)$$

with $a = \frac{1}{2} \sigma_1^2$, $b = r - \sigma_1^2 - \frac{1}{2} \rho \sigma_1 \sigma_2$ and $d = \frac{1}{2} \rho \sigma_1 \sigma_2 y$.

We want to approximate

$$g(\mathcal{V}) = a x \frac{\partial \mathcal{V}}{\partial x} + b \mathcal{V}$$

by a constant over $I_{x_1} = (0, x_1)$ satisfying the following two-point boundary value problem

$$\begin{cases} g'(v) = \left(a x \frac{\partial v}{\partial x} + b v \right)' = K_1 \\ v(0, y_j) = \mathcal{V}_{0,j} & v(x_1, y_j) = \mathcal{V}_{1,j} \end{cases} \quad (54)$$

By solving this problem we get

$$\mathcal{V} = \mathcal{V}_{0,j} + (\mathcal{V}_{1,j} - \mathcal{V}_{0,j}) \frac{x}{x_1} \quad (55)$$

Thereby, by using (52),(53), (54), (55) and the forward difference to approximate the first partial derivative $\frac{\partial \mathcal{V}}{\partial y}$ we get

$$\int_{(x_{\frac{1}{2}}, y_{j-\frac{1}{2}})}^{(x_{\frac{1}{2}}, y_{j+\frac{1}{2}})} \left(m_{11} \frac{\partial \mathcal{V}}{\partial x} + m_{12} \frac{\partial \mathcal{V}}{\partial y} + p\mathcal{V} \right) dy \approx \frac{1}{2} x_1 \left[\frac{1}{2} l_j (a+b) - d_j \right] \mathcal{V}_{i,1} + \frac{1}{2} d_j x_1 \mathcal{V}_{1,j+1} - \frac{1}{4} x_1 l_j (a-b) \mathcal{V}_{0,j} \quad (56)$$

where

$$a = \frac{1}{2} \sigma_1^2, \quad b = r - \sigma_1^2 - \frac{1}{2} \rho \sigma_1 \sigma_2 \quad d_j = \frac{1}{2} \rho \sigma_1 \sigma_2 y_j \quad l_j = y_{j+\frac{1}{2}} - y_{j-\frac{1}{2}}$$

Similarly, for the flux through the southern edge of the control volume $\mathcal{C}_{i,1}$ $i = 1, \dots, N$, we have

$$\int_{(x_{i-\frac{1}{2}}, y_{\frac{1}{2}})}^{(x_{i+\frac{1}{2}}, y_{\frac{1}{2}})} \left(m_{21} \frac{\partial \mathcal{V}}{\partial x} + m_{22} \frac{\partial \mathcal{V}}{\partial y} + q\mathcal{V} \right) dx \approx \frac{1}{2} y_1 \left[\frac{1}{2} h_i (e+k) - h'_i \right] \mathcal{V}_{i,1} + \frac{1}{2} h'_i y_1 \mathcal{V}_{i+1,1} - \frac{1}{4} y_1 h_i (e-k) \mathcal{V}_{i,0} \quad (57)$$

where

$$e = \frac{1}{2} \sigma_2^2, \quad k = r - \sigma_2^2 - \frac{1}{2} \rho \sigma_1 \sigma_2 \quad h'_i = \frac{1}{2} \rho \sigma_1 \sigma_2 x_i \quad h_i = x_{i+\frac{1}{2}} - x_{i-\frac{1}{2}}$$

3.2.4 The fitted L-Multi-Point Flux Approximation method (with the 1st order upwind method)

1. Fitted L-MPFA method (with 1st order upwind method)

Here the fitted finite volume method is combined with the first order upwind method . Thereby we have:

For the control volume \mathcal{C}_{11} , the western and southern edges of are (fully) in the degeneracy region. The integrals over the western and southern edges of the control volume \mathcal{C}_{11} are then approximated using the fitted finite volume (56) and (57). The integrals over the eastern and northern edges of the control \mathcal{C}_{11} , which are not in the degeneracy region, are approximated using the L-MPFA method coupled to the upwind method (1st and 2nd order).

$$\int_{\mathcal{C}_{11}} \nabla k(\mathcal{V}) d\mathcal{C}_{11} \approx aa_{11} \mathcal{V}_{11} + bb_{11} \mathcal{V}_{21} + cc_{11} \mathcal{V}_{22} + dd_{11} \mathcal{V}_{12} + ee_{11} \mathcal{V}_{01} + \beta\beta_{11} \mathcal{V}_{10}$$

where

$$aa_{11} = T_{11}^{22} + T_{34}^{21} + T_{41}^{22} + T_{22}^{12} + l_1 \max(f_x^2, 0) + h_1 \max(f_y^2, 0) - \frac{1}{2} x_1 \left(\frac{1}{2} l_1 (a+b) - d_1 \right) - \frac{1}{2} y_1 \left(\frac{1}{2} h_1 (e+k) - h'_1 \right)$$

$$bb_{11} = T_{33}^{21} + T_{12}^{22} + l_1 \min(f_x^2, 0) - \frac{1}{2} h'_1 y_1 \quad cc_{11} = T_{13}^{22} + T_{43}^{22}$$

$$dd_{11} = T_{23}^{12} + T_{44}^{22} + h_1 \min(f_y^2, 0) - \frac{1}{2} d_1 x_1 \quad ee_{11} = T_{21}^{12} + \frac{1}{4} l_1 x_1 (a-b)$$

$$\beta\beta_{11} = T_{31}^{21} + \frac{1}{4} y_1 h_1 (e-k)$$

Similarly, for the control volume $\mathcal{C}_{1,j}$ $j = 1, \dots, N$, only the southern edge is (fully) in the degeneracy region then the integral over it, is approximated using the fitted finite volume method (57). The integrals over the eastern, northern and western edges are approximated using the L-MPFA method coupled to the upwind methods(1st and 2nd order)

$$\int_{\mathcal{C}_{1,j}} \nabla \mathbf{k} \mathcal{V} d\mathcal{C}_{1,j} = aa_{1,j} \mathcal{V}_{1,j} + bb_{1,j} \mathcal{V}_{2,j} + cc_{1,j} \mathcal{V}_{2,j+1} + dd_{1,j} \mathcal{V}_{1,j+1} + \beta \beta_{1,j} \mathcal{V}_{1,j-1} + \alpha \alpha_{1,j} \mathcal{V}_{0,j-1} + ee_{1,j} \mathcal{V}_{0,j} \quad (58)$$

where

$$aa_{1,j} = T_{11}^{2,j+1} + T_{34}^{2,j} + T_{41}^{2,j+1} + T_{22}^{1,j+1} - T_{23}^{1,j} - T_{44}^{2,j} + l_j \max(f_x^2, 0) + h_1 \max(f_y^{j+1}, 0) - h_1 \min(f_y^j, 0) - \frac{1}{2} x_1 \left(\frac{1}{2} l_j (a + b) - d_j \right)$$

$$bb_{1,j} = T_{33}^{2,j} + T_{12}^{2,j+1} - T_{43}^{2,j} + l_j \min(f_x^2, 0) \quad cc_{1,j} = T_{13}^{2,j+1} + T_{43}^{2,j+1}$$

$$dd_{1,j} = T_{23}^{1,j+1} + T_{44}^{2,j+1} + h_1 \min(f_y^{j+1}, 0) - \frac{1}{2} d_j x_1 \quad \beta \beta_{1,j} = T_{31}^{2,j} - T_{22}^{1,j} - T_{41}^{2,j} - h_1 \max(f_y^j, 0)$$

$$\alpha \alpha_{1,j} = -T_{21}^{1,j} \quad ee_{1,j} = T_{21}^{1,j+1} + \frac{1}{4} l_j x_1 (a - b)$$

Using the same argument as above, for the control volume $\mathcal{C}_{i,1}$ $i = 2, \dots, N$, the integral over the southern edge is approximated using the fitted finite volume (57). The integrals over the eastern, northern and western edges are approximated using the L-MPFA method combined with the upwind methods (1st and 2nd order)

$$\int_{\mathcal{C}_{i,1}} \nabla (\mathbf{k} \mathcal{V}) d\mathcal{C}_{i,1} = aa_{i,1} \mathcal{V}_{i,1} + bb_{i,1} \mathcal{V}_{i+1,1} + cc_{i,1} \mathcal{V}_{i+1,2} + dd_{i,1} \mathcal{V}_{i,2} + ee_{i,1} \mathcal{V}_{i-1,1} + \alpha \alpha_{i,1} \mathcal{V}_{i-1,0} + \beta \beta_{i,1} \mathcal{V}_{i,0} \quad (59)$$

where

$$aa_{i,1} = T_{11}^{i+1,2} + T_{34}^{i+1,1} + T_{41}^{i+1,2} + T_{22}^{i,2} - T_{12}^{i,2} - T_{33}^{i,1} + l_1 \max(f_x^{i+1}, 0) + h_i \max(f_y^2, 0) - l_1 \min(f_x^i, 0) - \frac{1}{2} y_1 \left(\frac{1}{2} h_i (e + k) - h'_i \right)$$

$$bb_{i,1} = T_{33}^{i+1,1} + T_{12}^{i+1,2} + l_1 \min(f_x^{i+1}, 0) - \frac{1}{2} h'_i y_1 \quad cc_{i,1} = T_{13}^{i+1,2} + T_{43}^{i+1,2}$$

$$dd_{i,1} = T_{23}^{i,2} + T_{44}^{i+1,2} - T_{13}^{i,2} + h_i \min(f_y^2, 0) \quad ee_{i,1} = T_{21}^{i,2} - T_{11}^{i,2} - T_{34}^{i,1} - l_1 \max(f_x^i, 0)$$

$$\alpha\alpha_{i,1} = -T_{31}^{i,1} \quad \beta\beta_{i,1} = T_{31}^{i+1,1} + \frac{1}{4} y_1 h_i (e - k)$$

Besides, for the control volume \mathcal{C}_{ij} , $i, j = 2, \dots, N$, the L-MPFA method is used to approximate the diffusion term and the upwind to approximate the advection term. This leads to the following semi-discrete equation

$$\frac{d\mathcal{V}}{d\tau} = A\mathcal{V} + G(\mathcal{V}) + F \quad (60)$$

where

$$\mathcal{V} = \begin{bmatrix} \mathcal{V}_{11} \\ \mathcal{V}_{12} \\ \vdots \\ \mathcal{V}_{1N} \\ \mathcal{V}_{21} \\ \mathcal{V}_{22} \\ \vdots \\ \mathcal{V}_{NN} \end{bmatrix} \quad A = L^{-1} \left(Z + A_L \right) \quad G(\mathcal{V}) = \beta \left[\max(\mathcal{V}^* - \mathcal{V}, 0) \right]^{1/k}$$

with F the vector of boundary conditions, A_L a diagonal matrix of size $N \times N$ coming from the discretisation of (14). The diagonal elements of A_L are $A_{ii} = h_i l_i \lambda$ for $i = 1, \dots, N$ with λ given in (8). The matrix L is also a diagonal matrix of size $N \times N$ whose diagonal elements are $L_{ii} = h_i l_i$ for $i = 1, \dots, N$ and

$$Z = \begin{bmatrix} D_1 & K_1 & 0_N & \dots & \dots & \dots & \dots & 0_N \\ L_2 & D_2 & K_2 & \ddots & & & & \vdots \\ 0_N & L_3 & D_3 & K_3 & \ddots & & & \vdots \\ \vdots & \ddots & L_4 & D_4 & K_4 & \ddots & & \vdots \\ \vdots & & \ddots & \ddots & \ddots & \ddots & \ddots & \vdots \\ \vdots & & & \ddots & \ddots & \ddots & \ddots & 0_N \\ \vdots & & & & \ddots & L_{N-1} & D_{N-1} & K_{N-1} \\ 0_N & \dots & \dots & \dots & \dots & 0_N & L_N & D_N \end{bmatrix}$$

The elements of matrix Z are matrices. 0_N is a zeros matrix of size N . The matrices D_i, K_i, L_i are tri-diagonal matrices defined as follows:

$$\begin{aligned}
& \text{for } i = 1 \text{ or } i = N \\
& k = 1, \dots, N \quad (D_i)_{kk} = aa_{1,k} \quad k = 1, \dots, N-1 \quad (D_i)_{k,k+1} = dd_{1,k}, \quad k = 2, \dots, N \quad (D_i)_{k,k-1} = \beta\beta_{1,k} \\
& \text{for } i = 1 \quad k = 1, \dots, N \quad (K_1)_{kk} = bb_{1,k} \quad k = 1, \dots, N-1 \quad (K_1)_{k,k+1} = cc_{1,k} \\
& \text{for } i = N, \quad (L_N)_{11} = ee_{N,1} \quad k = 2, \dots, N \quad (L_N)_{kk} = e_{N,k} + \eta_{N,k} \quad k = 2, \dots, N \quad (L_N)_{k,k+1} = \alpha_{N,k} \\
& \text{for } i = 2, \dots, N-1 \\
& (D_i)_{11} = aa_{i,1}; \quad (D_i)_{12} = dd_{i,1}; \quad (K_i)_{11} = bb_{i,1}; \quad (K_i)_{12} = cc_{i,1} \quad (L_i)_{11} = ee_{i,1} \\
& k = 2, \dots, N \quad (D_i)_{kk} = a_{i,k} + \Omega_{i,k}; \quad (K_i)_{kk} = b_{i,k} + \Delta_{i,k}; \quad (L_i)_{kk} = e_{i,k} + \eta_{i,k} \\
& k = 2, \dots, N-1 \quad (D_i)_{k,k+1} = d_{i,k} + \phi_{i,k}; \quad (K_i)_{k,k+1} = c_{i,k} \\
& k = 2, \dots, N \quad (D_i)_{k,k-1} = \beta_{i,k} + \mu_{i,k}; \quad (L_i)_{k,k-1} = \alpha_{i,k}
\end{aligned}$$

where the elements $aa_{ij}, bb_{ij}, cc_{ij}, dd_{ij}, ee_{ij}, \beta\beta_{ij}$ are defined in (58),(58),(59), and the elements $a_{ij}, b_{ij}, c_{ij}, d_{ij}, e_{ij}, \Omega_{ij}, \Delta_{ij}, \beta_{ij}, \phi_{ij}, \alpha_{ij}, \mu_{ij}, \eta_{ij}$ are defined in (40) and (43).

2. Fitted Multi-Point Flux Approximation (2^{nd} order upwind)

Similarly, the fitted MPFA-L method deriving from the combination of the L-MPFA method and the 2^{nd} order upwind method leads to the following equation :

$$\frac{d\mathcal{V}}{d\tau} = A\mathcal{V} + G(\mathcal{V}) + F \quad (61)$$

where

$$\mathcal{V} = \begin{bmatrix} \mathcal{V}_{11} \\ \mathcal{V}_{12} \\ \vdots \\ \mathcal{V}_{1N} \\ \mathcal{V}_{21} \\ \mathcal{V}_{22} \\ \vdots \\ \mathcal{V}_{NN} \end{bmatrix} \quad A = L^{-1} \left(Y + A_L \right) \quad G(\mathcal{V}) = \beta \left[\max \left(\mathcal{V}^* - \mathcal{V}, 0 \right) \right]^{1/k}$$

with F the vector of boundary conditions. A_L is a diagonal matrix of size $N \times N$ coming from the discretisation of (14). The diagonal elements of A_L are $A_{ii} = h_i l_i \lambda$ for $i = 1, \dots, N$ with λ given in (8). The matrix L is also a diagonal matrix of size $N \times N$ whose diagonal elements are $L_{ii} = h_i l_i$ for $i = 1, \dots, N$

and

$$Y = \begin{bmatrix} H_1 & P_1 & R_1 & 0_N & \dots & \dots & \dots & \dots & 0_N & 0_N \\ Q_2 & H_2 & P_2 & R_2 & 0_N & & & & & 0_N \\ W_3 & Q_3 & H_3 & P_3 & R_3 & 0_N & & & & \vdots \\ 0_N & W_4 & Q_4 & H_4 & P_4 & R_4 & \ddots & & & \\ 0_N & 0_N & \ddots & \ddots & \ddots & \ddots & \ddots & \ddots & \ddots & \\ \vdots & & \ddots & \ddots & \ddots & \ddots & \ddots & \ddots & \ddots & \\ \vdots & & & \ddots & \ddots & \ddots & \ddots & \ddots & \ddots & 0_N \\ & & & & \ddots & W_{N-2} & Q_{N-2} & H_{N-2} & P_{N-2} & R_{N-2} \\ \vdots & & & & & \ddots & W_{N-1} & Q_{N-1} & H_{N-1} & P_{i,N-1} \\ 0_N & \dots & \dots & \dots & \dots & \dots & 0_N & W_N & Q_N & H_N \end{bmatrix}$$

The elements of matrix Y are matrices. 0_N is a zeros matrix of size N . The matrices H_i $i = 1, \dots, N$ are a penta-diagonal matrices and the matrices P_i, R_i, Q_i, W_i are diagonal matrices.

Furthermore, The θ - Euler method will be applied on the semi-discrete equations (45),(51), (60) and(61) for the spatial discretisation.

4 Time discretization

Let us consider the ODE stemming from the spatial discretization and given by (45),(51),(60) and(61)

$$\frac{d\mathcal{V}}{d\tau} = A\mathcal{V} + G(\mathcal{V}) + F$$

By using the θ -Euler method for the time discretization, we have

$$\text{for } m = 0, \dots, M \quad \frac{\mathcal{V}^{m+1} - \mathcal{V}^m}{\Delta\tau} = \theta \left(A\mathcal{V}^{m+1} + G(\mathcal{V}^{m+1}) + F(t_{m+1}) \right) + (1 - \theta) \left(A\mathcal{V}^m + G(\mathcal{V}^m) + F(t_m) \right) \quad (62)$$

At every time iteration, the nonlinear system where \mathcal{V}^{m+1} is the solution is solving using the Newton method. Note that

$$\mathcal{V}^m = [\mathcal{V}_{11}(\tau_m) \quad \mathcal{V}_{12}(\tau_m) \quad \dots \quad \mathcal{V}_{1N}(\tau_m) \quad \mathcal{V}_{21}(\tau_m) \quad \mathcal{V}_{22}(\tau_m) \quad \dots \quad \mathcal{V}_{2N}(\tau_m) \quad \dots \quad \mathcal{V}_{N,1}(\tau_m) \quad \mathcal{V}_{N,2}(\tau_m) \quad \dots \quad \mathcal{V}_{NN}(\tau_m)]^T$$

$$\tau_m = m\Delta\tau$$

where the time step is $\Delta\tau = \frac{T}{M}$, T being the maturity time.

5 Numerical experiments

In this section, we perform some numerical simulations for the L-MPFA method combined to the upwind methods (first and second order) and for the fitted L-MPFA method combined to the upwind methods (first and second order).

5.1 Errors for European call options

The computational domain of the problem is $\Omega = [0; 300] \times [0; 300] \times [0; T]$ with $T=1/12$. The numerical experiments are performed with the strike price $E = 100$, the volatilities $\sigma_1 = \sigma_2 = 0.3$, the correlation coefficient $\rho = 0.3$ and the risk free interest $r = 0.08$

Here, by taking $\beta = 0$ in (4), the L-MPFA method illustrated in the previous sections will be compared to the fitted finite volume method, Wang [2004], and the fitted O-MPFA methods for pricing multi-asset options for pricing options introduced in Koffi and Tambue [2019]. The relative error will be computed with respect to the analytical solution of the Black-Scholes PDE defined in Haug [2007] as follows

$$C(S_1, S_2, K, T) = S_1 e^{-rT} M(y_1, d; \rho_1) + S_2 e^{-rT} M(y_2, -d + \sigma\sqrt{T}; \rho_2) - K e^{-rT} \times \left(1 - M(-y_1 + \sigma_1\sqrt{T}, -y_2 + \sigma_2\sqrt{T}; \rho)\right) \quad (63)$$

where

$$d = \frac{\ln(S_1/S_2) + (b_1 - b_2 + \sigma_1^2/2)T}{\sigma\sqrt{T}},$$

$$y_1 = \frac{\ln(S_1/K) + (b_1 + \sigma_1^2/2)T}{\sigma_1\sqrt{T}}, \quad y_2 = \frac{\ln(S_2/K) + (b_1 + \sigma_2^2/2)T}{\sigma_2\sqrt{T}},$$

$$\sigma = \sqrt{\sigma_1^2 + \sigma_2^2 - 2\rho\sigma_1\sigma_2}, \quad \rho_1 = \frac{\sigma_1 - \rho\sigma_2}{\sigma}, \quad \rho_2 = \frac{\sigma_2 - \rho\sigma_1}{\sigma}$$

and

$$M(a, b; \rho) = \frac{1}{2\pi\sqrt{1-\rho^2}} \int_{-\infty}^a \int_{-\infty}^b \exp\left(-\frac{x^2 - 2\rho xy + y^2}{2(1-\rho^2)}\right) dx dy.$$

The solution using the L-MPFA coupled to the 2^{nd} order upwind method is illustrated as below

The L^2 -norm is used to compute the error is

$$err = \frac{\sqrt{\sum_{i,j=1}^N meas(\mathcal{C}_{ij})(\mathcal{V}_{ij} - V_{ij}^{ana})^2}}{\sqrt{\sum_{i=1}^n meas(\mathcal{C}_{ij})(V_{ij}^{ana})^2}} \quad (64)$$

where \mathcal{V} is the numerical solution, V^{ana} the analytical solution and $meas(\mathcal{C}_{ij})$ is the measure of the control volume \mathcal{C}_{ij} . This gives the following tables:

As we can observe in Table 1 and Table 2, the new fitted L-MPFA method is more accurate than the fitted O-MPFA method developed in Koffi and Tambue [2019] and the standard fitted finite volume method developed in Huang et al. [2006].

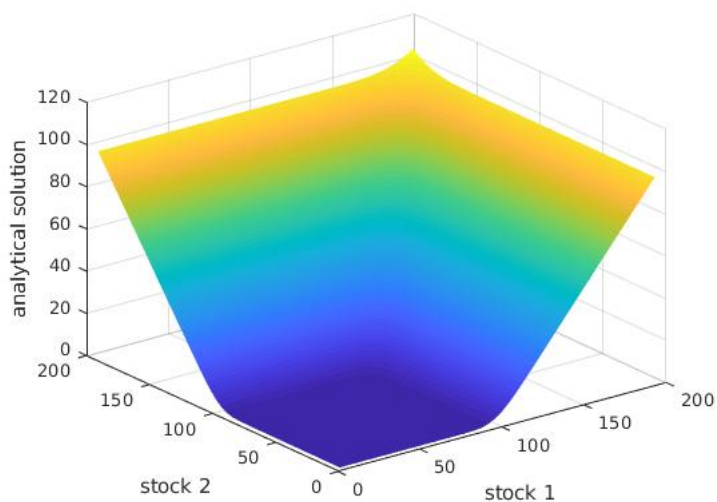
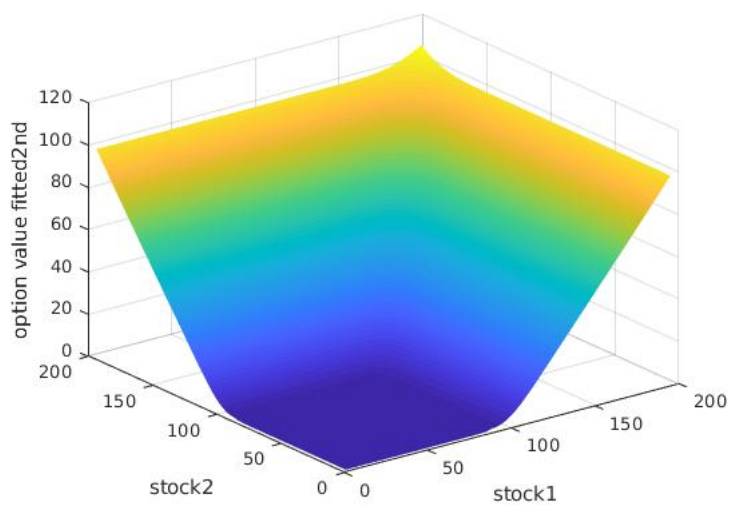


Fig. 7: Analytical solution

Fig. 8: L-MPFA -upwind 2^{nd} order

	Fitted fin vol	O-MPFA- 1^{st} upw	O-MPFA- 2^{nd} upw	fit O-MPFA- 1^{st} upw	fit O-MPFA- 2^{nd} upw
50×50	0.0317	0.0224	0.0225	0.0212	0.0212
70×70	0.0329	0.0248	0.0248	0.0238	0.0238
85×85	0.0327	0.0260	0.0260	0.0251	0.0251

Table 1: Table of errors

	L-MPFA- 1^{st} upw	L-MPFA- 2^{nd} upw	fit L-MPFA- 1^{st} upw	fit L-MPFA- 2^{nd} upw
50×50	0.0048	0.0049	0.0048	0.0047
70×70	0.0041	0.0041	0.0041	0.0041
85×85	0.0040	0.0040	0.0040	0.0040

Table 2: Table of errors

5.2 Errors for American put options

Since there is no analytical solution for the power penalty problem (4) for pricing American put options, and the numerical solution given by the fitted L-MPFA coupled to 2^{nd} order upwind method is more accurate when pricing European options (see Table 1 and Table 2), we have chosen for reference solution or "exact solution" the numerical solution given by the fitted L-MPFA coupled to 2^{nd} order upwind method with $dt = T/256$. The relative error of all the numerical methods used in this study will be performed with respect to this reference solution.

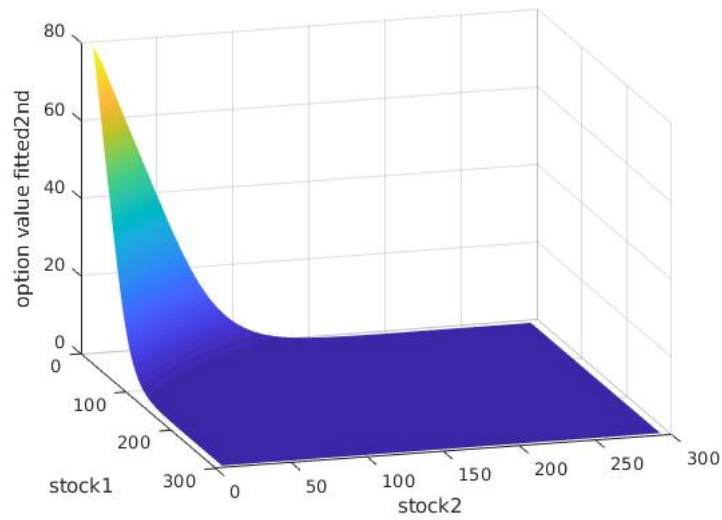


Fig. 9: Reference solution

For the numerical simulations below, the computational domain of the problem is $\Omega = [0; 300] \times [0; 300] \times [0; T]$ with $T = 1/6$, $K = 100$, the volatilities $\sigma_1 = \sigma_2 = 0.3$. The correlation coefficient is $\rho = 0.3$, the risk free interest $r = 0.08$. The penalty parameter $\beta = 256$ and the power penalty $k = 1/2$.

	Fitted Fin vol	L-MPFA-1 st upw	L-MPFA-2 nd upw	fit L-MPFA-1 st upw	fit L-MPFA -2 nd upw
50 × 50	0.0616	0.0610	0.0583	0.0611	0.0584
60 × 60	0.0277	0.0278	0.0276	0.0278	0.0277
70 × 70	0.0184	0.0183	0.0182	0.0182	0.0180
80 × 80	0.0104	0.0100	0.0098	0.0097	0.0095

Table 3: Table of errors for $\Delta\tau = T/64$

	Fitted Fin vol	L-MPFA-1 st upw	L-MPFA-2 nd upw	fit L-MPFA-1 st upw	fit L-MPFA -2 nd upw
50 × 50	0.0599	0.0520	0.0476	0.0522	0.0459
60 × 60	0.0227	0.0265	0.0249	0.0241	0.0220
70 × 70	0.0136	0.0148	0.0146	0.0146	0.0144
80 × 80	0.0087	0.0068	0.0065	0.0062	0.0059

Table 4: Table of errors for $\Delta\tau = T/128$

Again we can observe in Table 3 and Table 4, the novel fitted L-MPFA coupled to the 2^{nd} order upwind method is more accurate than the standard fitted finite volume by Huang et al. [2006].

6 Conclusion

In this paper, the L-MPFA methods have been introduced to approximate the diffusion term of the Black-Scholes PDE. The upwind methods (1^{st} and 2^{nd} order) are used for space discretization of the convection term appearing in the two dimensional Black-Scholes PDE. We have provided a novel scheme called the fitted L-MPFA method to handle the degeneracy of the Black Scholes PDE by combining the fitted finite volume and the L-MPFA method coupled to the upwind methods. Numerical experiments are performed and comparison between the L-MPFA methods, the O-MPFA methods by Koffi and Tambue [2019] and the fitted finite methods by Huang et al. [2006] are performed. The results have shown that the fitted L-MPFA method coupled to the 2^{nd} order upwind method is more accurate than the fitted finite volume by Huang et al. [2006] and the O-MPFA method by Koffi and Tambue [2019] for pricing Europeans and American options.

Acknowledgement

This work was supported by the Robert Bosch Stiftung through the AIMS ARETE Chair programme (Grant No 11.5.8040.0033.0).

References

- Ivar Aavatsmark. An introduction to multipoint flux approximations for quadrilateral grids. *Computational Geosciences*, 6(3-4):405–432 (2002).
- Ivar Aavatsmark. Multipoint flux approximation methods for quadrilateral grids. In *9th International forum on reservoir simulation, Abu Dhabi*, pages 9–13 (2007).
- Espen Gaarder Haug. *The complete guide to option pricing formulas*. McGraw-Hill Companies, 2007.
- C-S Huang, C-H Hung, and Song Wang. A fitted finite volume method for the valuation of options on assets with stochastic volatilities. *Computing*, 77(3):297–320 (2006).
- C-S Huang, C-H Hung, and Song Wang. On convergence of a fitted finite-volume method for the valuation of options on assets with stochastic volatilities. *IMA journal of numerical analysis*, 30(4):1101–1120 (2009).
- Pavlo Kovalov, Vadim Linetsky, and Michael Marozzi. Pricing multi-asset american options: A finite element method-of-lines with smooth penalty. *Journal of Scientific Computing*, 33(3):209–237(2007).
- Randall J LeVeque. Finite volume methods for hyperbolic problems. *Cambridge Texts in Applied Mathematics*, 39(1):88–89(2004).
- Rock S. Koffi, Antoine Tambue. A fitted multi-point flux approximation method for pricing two options. *Computational Economics (CSEM)*, <https://doi.org/10.1007/s10614-019-09906-x> (2019).
- Jürgen Topper. *Financial engineering with finite elements*, volume 319. John Wiley & Sons, 2005.
- S Wang, XQ Yang, and KL Teo. Power penalty method for a linear complementarity problem arising from american option valuation. *Journal of Optimization Theory and Applications*, 129(2):227–254 (2006).
- Song Wang. A novel fitted finite volume method for the black-scholes equation governing option pricing. *IMA Journal of Numerical Analysis*, 24(4):699–720 (2004).
- K Zhang, S Wang, X Yang, and Kok Lay Teo. A power penalty approach to numerical solutions of two-asset american options. *Numerical Mathematics: Theory, Methods and Applications*, 2:202–223 (2009).